Assessment of changes in stent graft geometry after chimney endovascular aneurysm sealing

Simon P. Overeem, MSc,[a,b] Seline R. Goudeketting, MSc,[a,b] Richte C. L. Schuurmann, PhD,[b,c] Jan M. Heyligers, MD, PhD,[d] Hence J. M. Verhagen, MD, PhD,[e] Michel Versluis, PhD,[b,f] *and* Jean-Paul P. M. de Vries, MD, PhD,[c] *Nieuwegein, Enschede, Groningen, Tilburg, and Rotterdam, The Netherlands*

ABSTRACT

Background: Chimney endovascular aneurysm sealing (ch-EVAS) could potentially minimize gutter-associated endoleaks in patients with juxtarenal abdominal aortic aneurysms resulting from the use of the conformable endobags surrounding the chimney stent grafts (ch-SGs). The aim of the present study was to quantify the (non)apposition of the endobags in the proximal aortic neck, migration of the endograft stent frames, and changes in geometry of the ch-SGs during the follow-up period.

Methods: The prospective data from 20 patients undergoing elective ch-EVAS were retrospectively reviewed. The aortic anatomy was analyzed on preoperative and postoperative computed tomography scans. The (non)apposition of the endobags in the aortic neck, Nellix (Endologix, Irvine, Calif) stent frame migration, and chimney graft geometry and migration were assessed.

Results: The median preoperative infrarenal neck length was 4.0 mm (interquartile range [IQR], 0-6.0 mm). The median seal length in the juxtarenal aortic neck at the first follow-up was 23.0 mm (IQR 18.0-30.8 mm). Five type IA endoleaks were identified on postoperative imaging; one at 1 month and four newly diagnosed at 1 year. Of these five type IA endoleaks, two were type Is1 (not extending into the aneurysm sac) and did not need reintervention and other three were type Is2 (extending into the aneurysm sac). One of these patients died of malignancy before reintervention could be performed. Bilateral ch-SG occlusions in one patient were documented at the 1-month follow-up (patient needed hemodialysis) and two patients with a new single ch-SG occlusion were found at the 1-year follow-up. No reinterventions were performed for the ch-SG occlusions. An occluded Nellix stent frame in one patient was treated with femorofemoral crossover bypass. Kaplan-Meier estimate of reintervention-free survival was 85.0% after 1 year. Migration ≥5 mm of the proximal end of the Nellix stent frames was observed in 20.0% of the patients, but no reintervention was performed at the 1-year follow-up. Imaging showed 20.1% of the available sealing surface was not used, and the nonapposition surface increased to 30.6% of the preoperative aortic neck surface at 1 year. Median migration was 3.5 mm (IQR, 2.4-5.0 mm) and 3.1 mm (IQR, 2.0-4.8 mm) for the left and right proximal end of the Nellix stent frames, respectively, and was 3.0 mm (IQR, 2.2-4.8 mm) for the proximal end of the ch-SGs at 1 year of follow-up.

Conclusions: Substantial distal migration of the Nellix endograft and positional changes of the ch-SGs in the juxtarenal aortic neck were observed at 1 year of follow-up, resulting in a 25.0% type IA endoleak rate, with three of these type IA endoleaks extending into the aneurysm sac. The reintervention-free survival rate was 85.0% at 1 year in this cohort of 20 patients. Careful follow-up after ch-EVAS is advised because changes are often subtle. The authors have stopped the ch-EVAS procedure so far. Long-term follow-up data on the stability of the Nellix endograft and the consequences of migration on ch-SGs is required before this technique should be used in clinical practice. (J Vasc Surg 2019;70:1754-64.)

Keywords: Abdominal aortic aneurysm; Chimney stent graft; Endovascular aneurysm sealing; EVAS; Nellix

The treatment of complex abdominal aortic aneurysms (AAAs) that involve the renal and visceral arteries has been challenging. A substantial number of patients with juxtarenal and pararenal AAAs will be unfit to undergo open repair. Therefore, endovascular interventions have been preferred. Although the short-term results of fenestrated endovascular aneurysm repair (f-EVAR) have been excellent, according to the GLOBALSTAR (Global Collaborators on Advanced Stent-Graft Techniques for Aneurysm Repair) registry,[1] a substantial proportion of patients will not be able to undergo f-EVAR because of anatomic issues.[2,3] Also, and the time required to manufacture these custom endografts can require ≤8 weeks.[2,3]

From the Department of Vascular Surgery, St Antonius Hospital, Nieuwegein[a]; the Multimodality Medical Imaging M3i Group, Technical Medical Centre,[b] and Physics of Fluids Group,[f] University of Twente, Enschede; the Division of Surgery, Department of Vascular Surgery, University Medical Centre Groningen, Groningen[c]; the Department of Vascular Surgery, Elisabeth TweeSteden Hospital, Tilburg[d]; and the Department of Vascular Surgery, Erasmus University Medical Center, Rotterdam.[e]

Author conflict of interest: J.M.H. is a consultant for Endologix.

Correspondence: Simon P. Overeem, MSc, Department of Vascular Surgery, St Antonius Hospital, Koekoekslaan 1, Nieuwegein 3435 CM, The Netherlands (e-mail: spovereem@gmail.com).

The editors and reviewers of this article have no relevant financial relationships to disclose per the JVS policy that requires reviewers to decline review of any manuscript for which they may have a conflict of interest.

0741-5214

https://doi.org/10.1016/j.jvs.2019.02.058

Off-the-shelf techniques, such as chimney EVAR (ch-EVAR), have been used for several years and have shown promising short-term results.[4-7] The disadvantages of the chimney technique include the formation of gutters and the increased risk of gutter-associated type IA endoleaks.[8] Chimney endovascular aneurysm sealing (ch-EVAS) has been introduced as technique similar to that of ch-EVAR, in which the uniqueness of the components potentially addresses one of the issues with parallel grafting (ie, gutters) using the conformable endobags of the Nellix Endosystem (Endologix, Irvine, Calif) to surround the chimney stent grafts (ch-SGs).[9-11]

To maximize the sealing length of the ch-EVAS configuration in the juxtarenal landing zone or the hereafter introduced apposition surface, the endobags of the Nellix endosystem must be deployed just below the orifice of the lowest unstented renal or visceral artery. To date, studies of the deployment accuracy of the Nellix endobags in the juxtarenal neck after ch-EVAS have been scarce, and little is known regarding the possible position changes of the Nellix stent frames, endobags, and ch-SGs during the follow-up period.

The aim of the present study was to quantify the non-apposition of the endobags in the juxtarenal aortic neck, determine the eventual migration of the endograft stent frames, and evaluate the changes in the geometry of the ch-SGs during ch-EVAS follow-up.

ARTICLE HIGHLIGHTS

- **Type of Research:** Multicenter retrospective cohort study
- **Key Findings:** Substantial distal migration of the Nellix endograft (Endologix, Irvine, Calif) and positional changes of the chimney stent grafts in the juxtarenal aortic neck were observed in 20 patients at 1 year, for a 25.0% type IA endoleak rate, with three of these cases extending into the aneurysm sac. The 1-year reintervention-free survival rate was 85.0%.
- **Take Home Message:** Careful follow-up after chimney endovascular aneurysm sealing is advised because the changes are often subtle. Long-term follow-up of the stability of the Nellix endograft and the consequences of migration on chimney stent grafts is required before this technique can be used in clinical practice.

METHODS

Patient population. A database containing the data from 27 consecutive patients who had undergone elective ch-EVAS patients from February 2015 to April 2017 was available from three high-volume endovascular departments. The institutional review board approved the present off-label and retrospective study, which was and compliant with the Declaration of Helsinki. Patient informed consent was not required in accordance with institutional policy on retrospective research. Two patients were excluded because of insufficient computed tomography (CT) contrast enhancement on the preoperative CT scans. Four patients had undergone duplex ultrasonography at the 1-year follow-up examination because of renal insufficiency and one patient had undergone evaluation with magnetic resonance angiography instead of CT angiography (CTA).These patients were excluded from the present analysis because the apposition software can only be used with CTA. Prospective data from the 20 remaining patients were analyzed retrospectively. Of these 20 patients, 14 had been previously included in a study of the early results and technical aspects of ch-EVAS.[11]

The American Society of Anesthesiologists physical status classification was class III for 12 of the 20 patients, who were, therefore, not good candidates for open repair mainly because of cardiopulmonary comorbidities. Of the remaining eight patients, with American Society of Anesthesiologists class II, five were considered to have a hostile abdomen because of previous abdominal surgery and three preferred endovascular treatment instead of open repair unless open repair could have been a good solution.

f-EVAR was not an option for several reasons. Of the 20 patients, 12 had unfavorable anatomy for f-EVAR owing to small iliac arteries (<6 mm) combined with severe atherosclerosis or a high juxtarenal angulation (>60°). Although an iliac conduit can be an option for patients with small external iliac arteries, this type of hybrid procedure was not the treatment of choice in the three hospitals. Percutaneous transluminal angioplasty with covered stent placement in these atherosclerotic iliac arteries was considered to be at high risk of stent occlusion during follow-up. Also, in some patients, the internal iliac artery had to be overstented, with ischemic consequences. The aneurysm in five patients was >6.5 cm, and a waiting time of ~6 to 8 weeks for a fenestrated device was judged to be too long a wait for these patients. These patients were treated within 3 weeks using ch-EVAS. For three patients, the physician's preference was to use a chimney procedure instead of an f-EVAR. Because ch-EVAR and ch-EVAS had not been approved by the Conformité Européenne at the time of treatment, the choice between the two techniques was at the discretion of a multidisciplinary endovascular team.

Procedure. The ch-EVAS technique used in the studied patients has been described by several investigators.[9-11] In most cases, access to the visceral and renal arteries was achieved through the left axillary or subclavian artery. To deliver the balloon-expandable covered ch-SGs (in most cases, the Atrium Advanta V12; Maquet Getinge Group, Mijdrecht, The Netherlands), the sheaths were placed over a Rosen Wire or fixed core guidewire (Cook

Medial Inc, Bloomington, Ind). The ch-SGs were slightly oversized (maximum, 1 mm) compared with the diameter of the branch arteries. During the procedure, the length of each ch-SG was measured, where the distal seal in the branch arteries was 10 to 15 mm, and the top of the ch-SGs was located just above the proximal bare end of the Nellix stent frames (Endologix, Irvine, Calif). After the ch-SGs had been positioned, the Nellix stent frames were introduced through the common femoral arteries. The Nellix stent frames were positioned such that the top of the frame was at the level of the intended proximal landing zone, and the proximal uncovered stent of the Nellix stent frame was located above the inferior border of the lowest unstented artery.

After deployment of the Nellix stent frames (Endologix), the endobags were prefilled with NaCl. The ch-SGs were deployed simultaneously. To avoid compression, the balloons in the ch-SGs were kept inflated during the prefill and subsequent polymer fill of the endobags, with a fill pressure of 180 to 200 mm Hg. An angiocatheter was advanced through the common femoral artery contralateral to the main body of the endograft. Digital subtraction angiography (DSA) was performed after the prefill and polymer fill, and the ch-SG balloons were deflated to check for endoleaks and ch-SG patency. In the case of endoleaks, the volume of the endobags was increased with an injection of polymer through the secondary fill line.

Imaging protocols. Preoperative and postoperative imaging studies from the ascending aorta to the common femoral arteries were available for all 20 patients. The postoperative imaging studies consisted of an arterial-phase CT scan with intravenous contrast and electrocardiographic gating at a 70% RR interval during the breath hold. Patients were scheduled for follow-up imaging studies at 1 and 12 months after the procedure.

The intraoperative DSA protocol was dependent on the patients' physique and renal function. DSA in the anteroposterior and lateral direction (or 60° right anterior oblique and 60° left anterior oblique angulations) was performed to check for type IA and IB endoleaks and stent–graft obstructions.

Three-dimensional imaging analysis. The aortic anatomy determined from the preoperative and postoperative CT scans was analyzed using 3Mensio Vascular, version 8.1, software (Pie Medical, Bilthoven, The Netherlands). On the preoperative CT scan, a center lumen line (CLL) was constructed at the midlumen to assess the neck geometry. On the postoperative scans, a CLL was constructed at the midlumen, through both Nellix stent frames (Endologix), and through each of the ch-SGs. The preoperative and postoperative measurements included the aortic neck diameter, infrarenal neck length, suprarenal and infrarenal angulation, maximum aneurysm diameter, and diameter of the ch-SGs. The measurements were performed independently by two experienced observers (S.O., S.G.).

Definitions. The definitions used in the present study were based on the Endologix's 2013 EVAS instructions for use (IFU), which were the indicated IFU during the period when the included patients had been treated. An infrarenal neck length of $<$10 mm was an indication for ch-EVAS.

Type IA and IB endoleak, Nellix stent frame (Endologix) occlusion, and ch-SG occlusion were considered major complications. We used the standard classification for EVAR procedures to classify type IA endoleak (endoleak distal to the proximal start of the fabric). However, the new EVAS type I classification, as defined by van den Ham et al,[12] was also determined.[12] A type Is1 has been defined as contrast enhancement found between the endobag and the aortic wall in the infrarenal neck but not reaching the aneurysm sac and not leading to reintervention. A type Is2 endoleak has been defined the appearance of contrast enhancement between the aneurysmal wall and endobag inside the aneurysm and meriting treatment.

The preoperative baseline was defined as the lower border of the lowest renal artery, perpendicular to the CLL. The target seal line was set at the lower border of the lowest unstented artery (Fig 1, *A*). In the case of a configuration with two renal ch-SGs, the target seal line was set at the lower border of the superior mesenteric artery (SMA). According to the IFU, a neck diameter of $\geq$32 mm was considered to be aneurysmal. The preoperative aortic neck surface was defined as the surface from the target seal line to that neck diameter (Fig 1, *A* and *B*). The Nellix endobags (Endologix) will seal the entire aneurysm; therefore, the postoperative aortic apposition surface will comprise the aneurysm sac. However, this can be an impractical and challenging definition to use in daily practice. Therefore, the postoperative nonapposition surface was defined as the surface between the target seal line and the upper circumference of the endobags sealing with the aortic wall (Fig 1, *C*).

(Non)apposition calculations. Markers were placed on the lower border of the renal and visceral arteries and four markers were placed on the proximal circumference of the endobags where full apposition with the aortic wall was achieved (Fig 2, *A*). A three-dimensional mesh of the aorta was exported from 3Mensio Vascular, version 8.1, software (Pie Medical), and the (non)apposition surface area (mm^2) between the Nellix endobags and the aortic wall was assessed using dedicated software, as described by Schuurmann et al.[13,14] To assess the changes in apposition during the follow-up period, the nonapposition surface area was analyzed as an absolute surface and as a percentage of the preoperative aortic neck surface area.

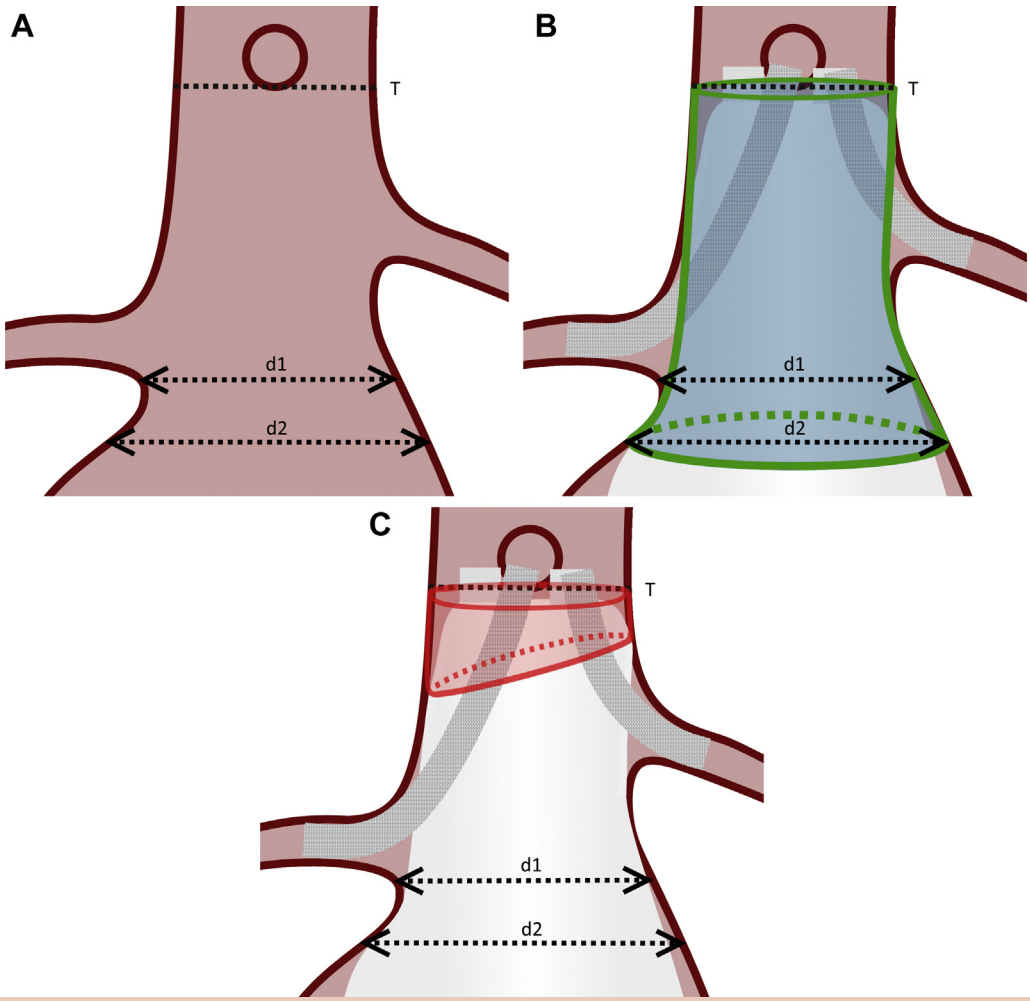

Fig 1. A, Definition of preoperative aortic neck surface: *d1* is baseline, *d2* is diameter ≥32 mm; target seal line (*T*) is set at the lower border of the lowest unstented artery. **B,** Theoretical preoperative sealing surface, from d2 up to the target seal line (*green*). **C,** Postoperative nonapposition surface from the circumference of the proximal endobags sealing with the aortic wall up to the lower border of the target seal line (*red*).

Migration of Nellix stent frames and ch-SGs. Dedicated software was used to quantify the migration of the Nellix stent frames, as described by van Veen et al.[15] Consecutive CT scans after ch-EVAS were aligned using rigid transformation and six fixed anatomic landmarks: the lower border of the SMA, both renal arteries, the aortic bifurcation, and the left and right iliac artery bifurcations. In the present study, only the migration of the proximal end of the Nellix stent frames (Endologix), relative to the SMA orifice, was determined. The root mean square error was calculated to find the error of the placement of the markers (mm) on the anatomic landmarks caused by differences in the quality of the CTA data sets, changes in anatomy, and the registration process.

The same method was used for the three-dimensional displacement of the ch-SGs. The migration of the proximal end of the ch-SG was of special interest because this part of the ch-SG will be fixed between aortic wall and Nellix endobag (Endologix). Therefore, migration of the Nellix endobags could result in migration of the proximal part of the ch-SGs. A reconstruction of Nellix stent frame migration and ch-SG migration is shown in Fig 2, *B*.

Geometry of ch-SGs. Two of us (S.P.O., S.R.G.) independently measured the ch-SG diameters. The ratio of the major and minor axis of the ch-SG (D ratio) was used to determine ch-SG compression.[16] A D ratio of 1 equals a circle, but higher values describe an oval shape and indicate ch-SG compression. The ch-SG angle (Fig 3, *A*) was defined as the angle between the visceral branch (ie, the vector on the CLL from the ostium to the most distal points along the CLL of the ch-SG) and the cross-sectional plane of the abdominal aorta at the level of the visceral artery ostium, derived from the methods used by Ullery et al.[17] The internal ch-SG angle (Fig 3, *B*) was defined as the angle between 2 directional vectors

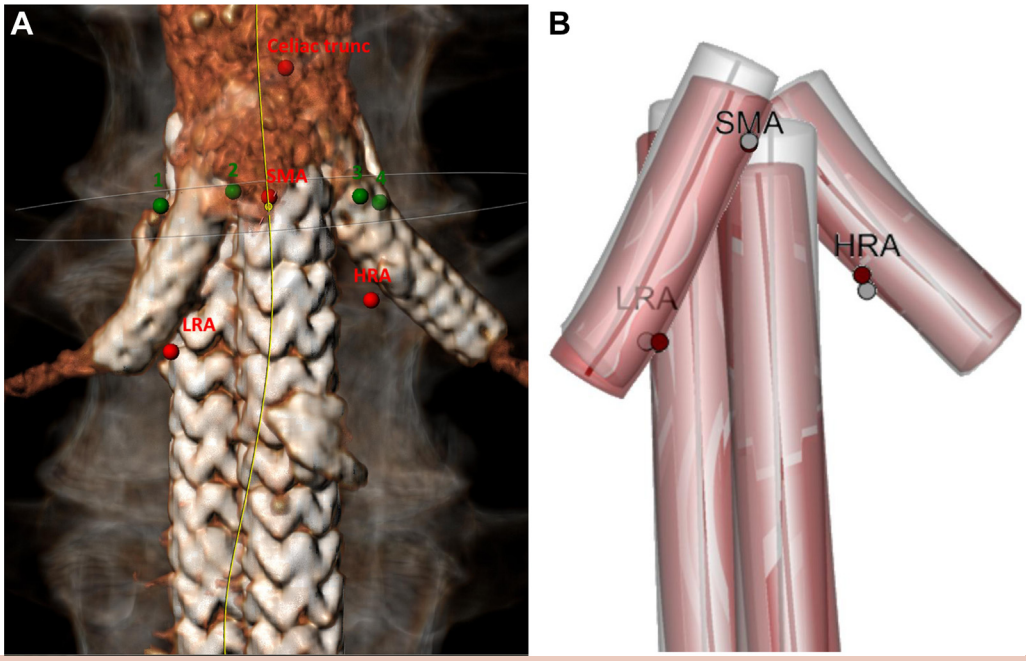

Fig 2. A, Reconstruction of Nellix stent frames and double chimney stent graft (ch-SG) configuration at 1-month follow-up (ie, ch-SGs in the left renal artery and superior mesenteric artery [SMA]). Reconstruction of Nellix stent frames and double ch-SG configuration at 1-month follow-up (ie, ch-SGs in both renal arteries). The *red markers*, needed for registration of the sequential computed tomography scans, are placed on the lower border of the celiac trunk, SMA, and highest (HRA) and lowest (LRA) renal artery. The *green markers*, needed to calculate the nonapposition surface, are located at the top of the circumference of the endobags (*markers 1-4*). The center lumen line (CLL) is shown in *yellow*. **B,** Anteroposterior reconstruction of the migration of the Nellix stent frames, left renal ch-SG, and right renal ch-SG, relative to the SMA orifice The stent frames of the Nellix and ch-SGs at 1 month (*gray*) and 1 year (*red*) after chimney endovascular aneurysm sealing. The red and gray dots represent the anatomic landmarks at the 1- and 12-month follow-up, aligned via rigid registration. The misalignment of the markers resulted from tissue deformation between the follow-up evaluations.

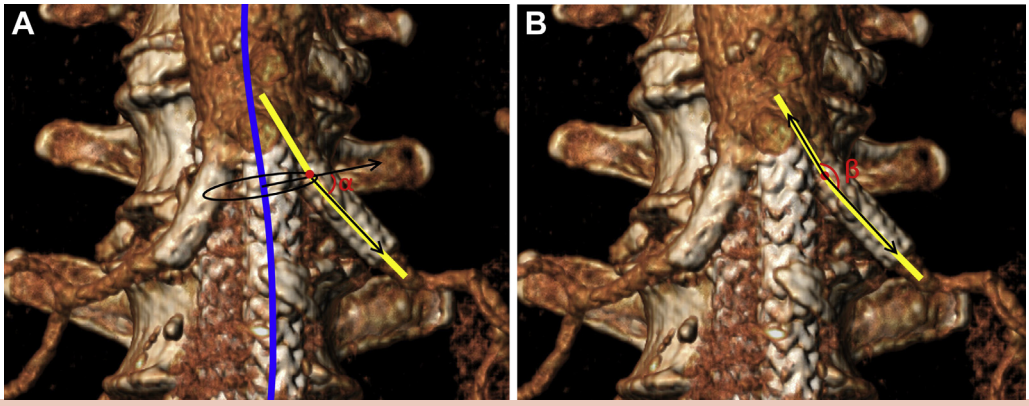

Fig 3. A, Chimney stent graft (ch-SG) angle (α) between the vector of cross-sectional plane of the abdominal aorta at the renal ostium and the vector of the ch-SG from the ostium to the most distal point on the centerline. **B,** Example of the internal ch-SG angle (β) between the ch-SG in the lumen and the ch-SG in the vessel. The center lumen line (CLL) of the ch-SG is shown in *yellow*.

over the CLL of the ch-SG. Both vectors started at the point on the ch-SG CLL closest to the ostium and ended at the proximal or distal end of the ch-SG.

Statistical analysis. Statistical analysis was performed using SPSS, version 25, software (IBM Corp, Armonk, NY). Continuous variables are expressed as the median and interquartile range (IQR). The interobserver agreements were determined for the (non)apposition, neck diameters, and ch-SG geometry parameters of the first 10 CTA studies. Interobserver agreement was tested using the intraclass correlation coefficient (ICC), a two-way mixed model by absolute agreement. The ICC values were interpreted in levels of agreement assessed as poor (0-0.20), fair

Table I. Patient and aneurysm characteristics

Characteristic	Median [IQR]
Patients, No.	20
Age, years	75.9 [9.1]
Sex, n	
Male	16
Female	4
ASA score, No.	
II	8
III	12
Preoperative aneurysm characteristics, mm	
AAA diameter	62.4 [8.8]
Neck diameter baseline	31.9 [7.0]
Neck diameter at SMA	28.8 [2.9]
Neck diameter at celiac trunk	29.2 [3.1]
Infrarenal neck length	4.0 [6.0]
Chimneys used, No.	
1 ch-SG	8 (renal ch-SGs)
2 ch-SGs	11 (19 renal ch-SGs, 3 SMA ch-SGs)
3 ch-SGs	1 (2 renal ch-SGs, 1 SMA ch-SG)
Stent name	
Atrium Advanta V12[a]	26
Gore Viabahn[b]	3
LIFESTREAM[c]	3
Chromis[d]	1

AAA, Abdominal aortic aneurysm; *ASA*, American Society of Anesthesiologists (physical status classification); *ch-SG*, chimney stent graft; *IQR*, interquartile range; *SMA*, superior mesenteric artery.
[a]Maquet Getinge Group, Rastatt, Germany.
[b]Gore Medical, Flagstaff, Ariz.
[c]C.R. Bard, New Providence, NJ.
[d]Medtronic, Dublin, Ireland.

(0.21-0.40), moderate (0.41-0.60), good (0.61-0.80), and perfect (0.81-1) with the 95% confidence intervals (CIs). Differences in ch-SG angulation and ch-SG migration between follow-up evaluations were tested using a Wilcoxon signed rank test. *P* values were considered significant at a 2-tailed α of $<.05$. A linear regression analysis was performed to determine whether Nellix stent frame migration and the corresponding ch-SG migration were associated.

RESULTS

The patient demographic data and in-hospital, 30-day, and 1-year complications are reported in Table I. A mean number of 1.7 ch-SGs were implanted per patient. Of the 20 patients, eight were treated with 1 ch-SG, 11 with 2 ch-SGs, and 1 with a triple ch-SG configuration. The median neck length at the first follow-up examination was 23.0 mm (IQR, 18.0-30.8 mm). Hence, when the preoperative neck length was considered, the theoretical gain in neck length with the use of ch-SGs would be 19.0 mm.

Interobserver agreement. The ICCs were 0.990 (95% CI, 0.957-0.998) for the nonapposition surface (n = 10), 0.960 (95% CI, 0.945-0.972) for the neck diameter (n = 140), and 0.917 (95% CI, 0.899-0.931) for the ch-SG diameter measurements (n = 380).

Nonapposition. The median preoperative aortic neck surface for all patients was 2611.5 mm^2 (IQR, 1436.9-3091.1 mm^2). The median nonapposition surface at the first follow-up evaluation was 525.0 mm^2 (IQR, 285.3-1172.9 mm^2), indicating that 20.1% of the available sealing surface was not used. At the 1-year follow-up examination, the median nonapposition surface had increased to 799.4 mm^2 (IQR, 450.0-1403.8 mm^2), or 30.6% of the preoperative aortic neck surface. The baseline diameter remained constant during follow-up (1-month follow-up, 31.9 mm [IQR, 28.2-34.0 mm]; 12-month follow-up, 31.8 mm [IQR, 30.1-36.0 mm]). A typical example is shown in Fig 4.

Migration of stent frames. The median distal migration of the proximal end of the left and right Nellix stent frames (Endologix) was comparable at 3.5 mm (IQR, 2.4-5.0 mm) vs 3.1 mm (IQR, 2.0-4.8 mm). The median root mean square error was 1.4 mm (IQR, 1.3-1.5 mm). The amount of migration was ≥5 mm for 5 Nellix stent frames in 4 patients (20.0%).

Geometry of ch-SGs. The median distal migration of the proximal end of the ch-SGs (3.0 mm [IQR, 2.2-4.8 mm]) differed significantly from the migration of the distal ending (1.7 mm [IQR, 0.0-3.4 mm]; $P < .001$) between follow-up assessments. Migration of ≥5 mm had occurred in 8 ch-SGs (6 renal ch-SGs and 2 SMA ch-SGs) in 6 patients. The ch-SG geometry results are reported in Table II. Although the ch-SG angulation and D ratio did not differ significantly during the follow-up period, the median internal ch-SG angulation had changed by 4.3° during the follow-up period ($P = .021$). Thus, the proximal ending of the renal ch-SG had shifted mostly distally.

Four ch-SGs (12.1%) became occluded during the follow-up period (Table III). Analysis of the ch-SG diameter showed compression (D ratio, >2) in 15.2% of the ch-SGs and 25.0% of the patients. In this cohort, no significant association was found between ch-SG compression and ch-SG occlusion. Some patients showed high compression rates (D ratio, >3); however, the ch-SG remained patent and the other ch-SGs had become occluded without any compression.

Complications and reinterventions. Type IA and IB endoleak, stent frame occlusion, and ch-SG occlusion were considered as major complications and occurred in eight patients within 1 year after the procedure (Table III). Five type IA endoleaks were identified on postoperative

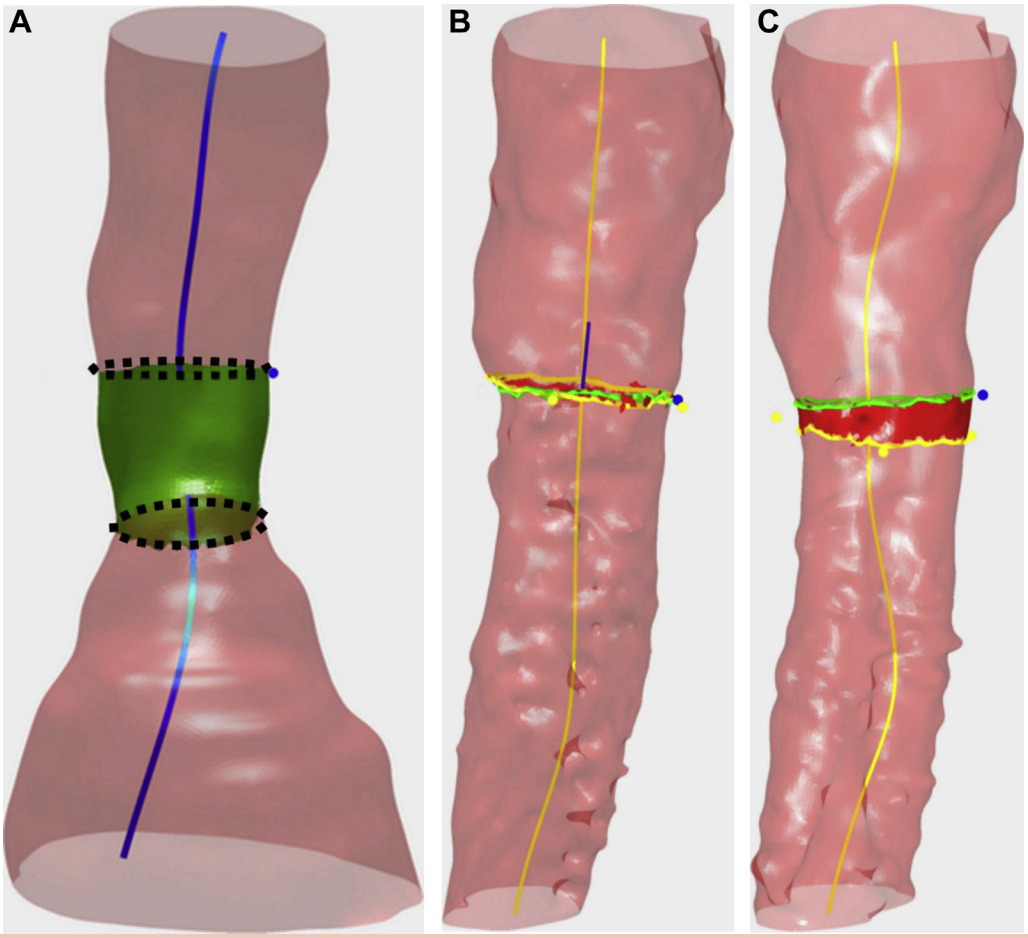

Fig 4. A, Typical example of a patient treated with a single chimney stent graft (ch-SG) for the right renal artery. The preoperative aortic neck surface is shown in *green* (2327.3 mm^2). The *upper dotted line* is the target seal line, set at the highest renal artery; the *lower dotted line* is the aortic neck diameter (>32 mm). **B,** Nonapposition surface area at the 1-month follow-up examination shown in *red* (49.2 mm^2). **C,** Nonapposition surface area at 12 month follow-up examination shown in *red* (268.0 mm^2).

imaging: one at 1 month and four newly diagnosed at 12 months. Of these five type IA endoleaks, two were type Is1 and did not require reintervention. Careful observation of these patients during the follow-up period is recommended, because Is1 leaks are prone to progression and, sometimes, a small type IA endoleak could be overlooked, as described by van den Ham et al.[12] The three other type IA endoleaks were type Is2 (extending into the aneurysm sac). One of these patients died of malignancy before reintervention could be performed. Bilateral ch-SG occlusion in one patient was documented at the 1-month follow-up examination (the patient required hemodialysis), and new single ch-SG occlusion in two patients was found at the 1-year follow-up evaluation. No reintervention was performed on any of the ch-SG occlusions. An occluded Nellix stent frame in one patient was treated with femorofemoral crossover bypass. The crossover bypass had occluded after 11 months; however, no reintervention of the bypass was performed because the patient had experienced mild complaints. The freedom from major complications was 60%, and the freedom from reinterventions was 85% (Fig 5).

DISCUSSION

In the present series of 20 patients undergoing elective ch-EVAS with 1-year CTA follow-up, positional changes in Nellix stent frames, ch-SGs, and apposition between the endobags and the juxtarenal aortic wall was determined using dedicated software. Theoretically, the Nellix endosystem offers a circumferential seal to minimize gutter-associated endoleaks, the Achilles' heel of ch-EVAR. However, a type IA endoleak occurred in one quarter of the patients in the present series, and the risk of complications was substantial. Most of the existing data regarding ch-EVAS have come from case reports or very small retrospective series. Only 1 large ch-EVAS registry has been reported to date. Thompson et al[9] showed good short-term results in the Aneurysm Study for

Table II. Geometry of chimney stent graft

Variable	Follow-up examination	
	1 Month	12 Months
Renal arteries		
ch-SG angulation, °	37.3 [19.4]	35.8 [24.6]
Internal ch-SG angulation, °	151.1 [20.7]	155.4 [21.6]
Average D ratio ± SD	1.1 ± 0.2	1.1 ± 0.2
Maximum D ratio ± SD	1.4 ± 0.5	1.4 ± 0.2
Superior mesenteric arteries		
ch-SG angulation, °	40.6 ± 8.4	39.4 ± 10.9
Internal ch-SG angulation, °	160.9 [13.9]	160.8 [11.5]
Average D ratio ± SD	1.2 ± 0.3	1.3 ± 0.1
Maximum D ratio ± SD	1.5 ± 0.7	1.7 ± 0.3

ch-SG, Chimney stent graft; *D ratio*, ratio of the major and minor axis of the chimney stent graft; *SD*, standard deviation.
Data are presented as median [interquartile range], unless noted otherwise.

Table III. Complications and reinterventions during follow-up

Pt. No.	1-Month follow-up evaluation		12-Month follow-up evaluation	
	Complication	Reintervention	Complication	Reintervention
2	None	NA	Type IA endoleak[a]	No
3	None	NA	Type IA endoleak[a]; occlusion of left renal artery ch-SG	No
4	None	NA	Type IA endoleak[b]	Onyx embolization
7	Occlusion of right Nellix stent frame	Femorofemoral crossover	Occlusion of femorofemoral crossover	No
11	Type IA endoleak[b]	Embolization with coils IMA	None	NA
14	None	NA	Type IA endoleak[b,c]	No
17	Occlusion of both renal artery ch-SGs, leading to hemodialysis	No	None	NA
19	None	NA	Occlusion of left renal artery ch-SG	No

ch-SG, Chimney stent graft; *IMA*, inferior mesenteric artery; *NA*, not applicable; *Pt. no.*, patient number.
[a]Type Is1 endoleak, not extending into the aneurysm sac and, therefore, not treated.
[b]Type Is2 endoleak, contrast enhancement between the endobag and aneurysmal wall or thrombus inside the aneurysm sac, meriting treatment.
[c]Died of malignancy, not related to endovascular aneurysm sealing (15 months after treatment), before reintervention.

Complex AAA, Evaluation of Nellix Durability (ASCEND) registry (n = 154). At 1 year, freedom from type IA endoleak was 95.7%, and freedom from reinterventions was 89.2%. Waiting for the midterm and long-term results of this registry before implementing the technique on a large scale seems appropriate. We have, thus, stopped performing the ch-EVAS procedure, especially because good alternatives are available, such as open surgery, f-EVAR, and, even, ch-EVAR, all with proven good midterm outcomes.[7,18,19]

Nonapposition surface. The (non)apposition surface area in the aortic neck has been introduced to describe the sealing zone of the Nellix endosystem (Endologix) more accurately (Fig 2, *B*). The findings from standard CTA can report only on the state the position of the stent frames, and no information on the position of the endobags is provided. The (non)apposition method quantifies the position and apposition of the endobags, as well as any small changes in these parameters during the follow-up period. In three patients, the non-apposition surface as a percentage of the preoperative aortic neck surface at the 1-month follow-up was >50% (55.0%, 59.0%, and 86.0%, respectively). At the 12-month follow-up examination, the nonapposition surface for these patients had increased to 59.5%, 90.4%, and 100%, respectively. These patients had an angulated neck (>60° infrarenal angulation), with the Nellix stent frames positioned in the outer curve. These challenging neck characteristics might have resulted in a poor position of

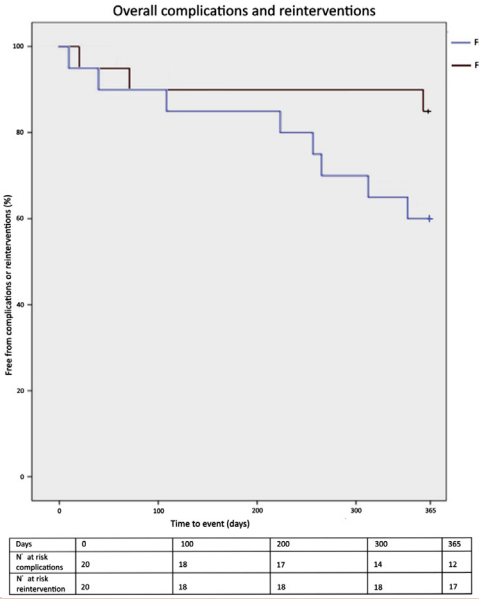

Fig 5. Kaplan-Meier curves for freedom from major complications (*blue*) and freedom from reintervention (*red*).

the endobags and minimal filling with polymer and, therefore, nonapposition. In 1 patient, the Nellix stent frames buckled in opposite directions, leading to a type Is2 endoleak.

At the first postoperative CTA, 20.0% of the available apposition surface was not sealed with the endobags. To avoid incomplete sealing owing to hanging shoulders of the endobags, the stent frames must be positioned 5 mm above the target seal line, which might seem counterintuitive compared with EVAR procedures. Furthermore, no markers are set at the top of the endobags, making accurate positioning more difficult. To identify the position of the top and sides of the endobags during the procedure, contrast in the prefill is needed. If the endobags appear to be too high, the prefill can be removed and the stent frames repositioned. Using this strategy might minimize the risk for occluding a side branch at the seal line. Sufficient filling of the endobags, using a fill pressure of 180 mm Hg (according to the IFU), should be enough to prevent an irregular shape at the top of the endobags. Nevertheless, the physician must be aware that the top of the endobags will not always be flat.

To identify the target seal line during ch-EVAS, the C-arm should be positioned in a lateral and an anteroposterior direction. In the case of a 2 ch-SG configuration, lateral DSA is crucial to identify the target seal line at the lower border of the SMA.

Migration. No consensus has been reached on the definition of device migration in the reported data.[20,21] The most commonly used cutoff definition (Society for Vascular Surgery) has been >10 mm. van Veen et al,[15] England et al,[22] and Dorweiler et al[23] recently reported new methods to detect device migration accurately, using a cutoff value of ≥5 mm, ≥4 mm, and ≥2 mm, respectively. Detection of 5-mm migration seems crucial, because all the Nellix migrations were <10 mm but led to substantial migration of a considerable part of the ch-SGs.

Migration was measured for the proximal and distal ends of the ch-SG. To minimize motion artifact of the ch-SGs, CTA was acquired during the arterial phase in breath hold. Migration of the proximal end of the ch-SG was significantly larger than that of the distal end of the ch-SG in our cohort.

ch-SG geometry. No consensus has been reached on the best method of positioning ch-SGs during parallel stenting. Several investigators have studied the outcomes with different techniques of treating complex aneurysms as a result of branch geometry.[17,24-26] Inherent to the parallel stenting technique is the sharp angulation of the ch-SG (ie, small internal angle) because the ch-SG is placed parallel to the endograft. In ch-EVAS, the ch-SG is not necessarily positioned parallel to the endobag and vessel wall owing to the conformable endobags, resulting in a relatively large (151°) internal angle. Positioning ch-SGs alongside the endograft during parallel stenting will result in a different perfusion rate of the visceral and renal branches compared with using flared endografts during f-EVAR.[27]

During the follow-up period, 12.1% of the ch-SGs became occluded compared with 2.7% in the ASCEND registry.[9] If kinking or compression of the ch-SG is seen, adding a self-expandable ch-SG might be a good solution to prevent occlusion of the ch-SG. Boersen et al[28] showed in an in vitro study that vortices occur proximal to the endobags, especially in wider necks, which has been associated with thrombus formation.[29] Thrombi can be directed into the ch-SG and can lead to occlusion. Dual-platelet therapy could be indicated after ch-EVAS, although clinical evidence regarding the administration of platelet inhibitors after the implantation of stent grafts is still lacking.[30]

Software. The present retrospective study with a small number of patients found no clinical benefits could be gained with the software. These new measurements have two possible advantages. First, the measurements can serve as a precise determination of the postoperative seal in the juxtarenal or infrarenal neck at the first postoperative CT scan. Second, because the geometric changes are often subtle, the post-EVAS image analysis software should be able to detect (subtle) changes in endobag and stent graft position over time. One of the particular problems with EVAS is that the endobags are not oversized compared with the diameter of the aortic neck. In the case of dilatation of the infra- or juxtarenal

aortic neck, the endobags could lose circumferential apposition and, thus, seal, even when the stent grafts or endobags do not migrate. This loss of apposition can be difficult to detect with standard arterial-phase CT with intravenous contrast analysis. Therefore, we advocate the use of the new imaging software, which can determine small changes in the loss of apposition. A comparison of the amount of nonapposition on consecutive post-EVAS CT scans during follow-up can, thus, be helpful in the detection of possible seal problems. Validation of this dedicated apposition and migration software in patients with EVAR was recently reported.[13] The new measurements enabled the detection of subtle changes in endograft dimensions on regular CT scans in many patients before the complication became urgent.[14]

Linear measurements of neck length, from the orifice of the lowest renal artery to the proximal top of the fabric along the aortic wall, have been used to define the neck seal in EVAR. However, if applied in EVAS, these measurements would not consider the irregular shape of the top of the Nellix endobags. The endobags in some patients will have a flat top; however, the endobags in others can have so-called hanging shoulders.[31] In addition, the left and right endobags will not be positioned at equal height in most patients. This is especially true for those with angulated necks, for which the stent frame of the Nellix endobag in the outer curve can be deployed higher to increase the seal length in the aortic neck. Measuring the distance between the target seal line and the top of the stent frames to describe the seal zone would be inaccurate because the distance between the top of the stent frame and the top of the endobags is not fixed. In addition, movement between the stent frame and endobag can occur, which could result in a missed migration event of the endobags during follow-up if only neck length has been used.

The (non)apposition surface is not a parameter that can be used for direct comparison between patients owing to differences in the neck diameter. The nonapposition surface, as a percentage of the preoperative neck surface, can be used to compare differences during the follow-up period. Combining this information with stent frame migration will provide a full determination of the changes in the position of the Nellix endosystems (Endologix).

Study limitations. The limitations of the present study included the relative small number of patients, the use of 4 different types of ch-SGs, and the short follow-up period. In the present analysis, we did not consider the orientation of the ch-SGs as a potential contributor to gutter-related endoleak.

The median juxtarenal neck diameters were within the requirements of the 2013 IFU; however, the 2016 IFU restricted the use of the Nellix endosystem to neck diameters <28 mm.[32] This might explain the high incidence of major complications, because some necks would have been considered aneurysmal according to the 2016 IFU.

Although the use of duplex ultrasound imaging during follow-up has several benefits, CT imaging during follow-up remains necessary for the dedicated software. No dynamic CTA scans were made; therefore, changes in geometry during the cardiac cycle were not analyzed.

CONCLUSIONS

Careful follow-up after ch-EVAS is advised because the changes are often subtle. The new software could help to better determine the position and apposition of the endobags and to register eventual changes in sealing during the follow-up period. Substantial distal migration of the Nellix endograft and positional changes of the ch-SGs in the juxtarenal aortic neck were observed at the 1-year follow-up evaluations. This resulted in a 25.0% rate of type IA endoleak, with 3 of these type IA endoleaks extending into the aneurysm sac. The reintervention-free survival rate was 85.0% at 1 year, and the major complication rate was 40% in this cohort of 20 patients. We have stopped using the ch-EVAS procedure until additional data are available. Long-term follow-up evaluating the stability of the Nellix endograft and the consequences of migration on ch-SGs is required, as are the long-term results from the ASCEND registry before this technique should be used in clinical practice.

AUTHOR CONTRIBUTIONS

Conception and design: SO, JV
Analysis and interpretation: SO, SG, RS, MV, JV
Data collection: SO, SG, JH, HV
Writing the article: SO, SG, JV
Critical revision of the article: SO, SG, RS, JH, HV, MV, JV
Final approval of the article: SO, SG, RS, JH, HV, MV, JV
Statistical analysis: SO
Obtained funding: Not applicable
Overall responsibility: SO

REFERENCES

1. British Society for Endovascular Therapy and the Global Collaborators on Advanced Stent- Graft Techniques for Aneurysm Repair (GLOBALSTAR) Registry. Early results of fenestrated endovascular repair of juxtarenal aortic aneurysms in the United Kingdom. Circulation 2012;125:2707-15.
2. Schanzer A, Simons JP, Flahive J, Durgin J, Aiello FA, Doucet D, et al. Outcomes of fenestrated and branched endovascular repair of complex abdominal and thoracoabdominal aortic aneurysms. J Vasc Surg 2017;66:687-94.
3. Oderich GS, Ribeiro M, Hofer J, Wigham J, Cha S, Chini J, et al. Prospective, nonrandomized study to evaluate endovascular repair of pararenal and thoracoabdominal aortic aneurysms using fenestrated-branched endografts based on supraceliac sealing zones. J Vasc Surg 2017;65:1249-59.e10.
4. Donas KP, Torsello GB, Piccoli G, Pitoulias GA, Torsello GF, Bisdas T, et al. The PROTAGORAS study to evaluate the performance of the Endurant stent graft for patients with

pararenal pathologic processes treated by the chimney/snorkel endovascular technique. J Vasc Surg 2016;63:1-7.
5. Bruen KJ, Feezor RJ, Daniels MJ, Beck AW, Lee WA. Endovascular chimney technique versus open repair of juxtarenal and suprarenal aneurysms. J Vasc Surg 2011;53:895-905.
6. Patel RP, Katsargyris A, Verhoeven ELG, Adam DJ, Hardman JA. Endovascular aortic aneurysm repair with chimney and snorkel grafts: indications, techniques and results. Cardiovasc Intervent Radiol 2013;36:1443-51.
7. Donas KP, Lee JT, Lachat M, Torsello G, Veith FJ. Collected world experience about the performance of the snorkel/chimney endovascular technique in the treatment of complex aortic pathologies. Ann Surg 2015;262:546-53.
8. Overeem SP, Boersen JT, Schuurmann RCL, Groot Jebbink E, Slump CH, Reijnen MMPJ, et al. Classification of gutter type in parallel stenting during endovascular aortic aneurysm repair. J Vasc Surg 2017;66:594-9.
9. Thompson M, Youssef M, Jacob R, Zerwes S, Reijen MMPJ, Szopinski P, et al. Early experience with endovascular aneurysm sealing in combination with parallel grafts for the treatment of complex abdominal aneurysms: the ASCEND registry. J Endovasc Ther 2017;24:764-72.
10. Torella F, Chan TY, Shaikh U, England A, Fisher RK, McWilliams RG. ChEVAS: combining suprarenal EVAS with chimney technique. Cardiovasc Intervent Radiol 2015;38:1294-8.
11. Dinkelman MK, Overeem SP, Boeckler D, De Vries JPPM, Heyligers JMM. Chimney technique in combination with a sac-anchoring endograft for juxtarenal aortic aneurysms: technical aspects and early results. J Cardiovasc Surg (Torino) 2016;57:730-6.
12. van den Ham LH, Holden A, Savlovskis J, Witterbottom A, Ouriel K, Reijnen MMPJ, et al. Editor's choice—occurrence and classification of proximal type I endoleaks after endovascular aneurysm sealing using the Nellix^{TM} device. Eur J Vasc Endovasc Surg 2017;54:729-36.
13. Schuurmann RCL, Overeem SP, van Noort K, de Vries BA, Slump CH, de Vries J-PPM. Validation of a new methodology to determine 3-dimensional endograft apposition, position, and expansion in the aortic neck after endovascular aneurysm repair. J Endovasc Ther 2018;25:358-65.
14. Schuurmann RCL, van Noort K, Overeem SP, van Veen R, Ouriel K, Jordan WD, et al. Determination of endograft apposition, position, and expansion in the aortic neck predicts type Ia endoleak and migration after endovascular aneurysm repair. J Endovasc Ther 2018;25:366-75.
15. van Veen R, van Noort K, Schuurmann RCL, Wille J, Slump CH, de Vries J-PPM. Determination of stent frame displacement after endovascular aneurysm sealing. J Endovasc Ther 2017;25:52-61.
16. Overeem SP, Donselaar EJ, Boersen JT, Groot Jebbink E, Slump CH, de Vries JPPM, et al. In vitro quantification of gutter formation and chimney graft compression in chimney EVAR stent-graft configurations using electrocardiography-gated computed tomography. J Endovasc Ther 2018;25:387-94.
17. Ullery BW, Suh G, Lee JT, Liu B, Stineman R, Dalman R, et al. Comparative geometric analysis of renal artery anatomy before and after fenestrated or snorkel/chimney endovascular aneurysm repair. J Vasc Surg 2016;63:922-9.
18. Katsargyris A, Oikonomou K, Klonaris C, Töpel I, Verhoeven ELG. Comparison of outcomes with open, fenestrated, and chimney graft repair of juxtarenal aneurysms: are we ready for a paradigm shift? J Endovasc Ther 2013;20:159-69.
19. van Lammeren GW, Ünlü Ç, Verschoor S, van Dongen EP, Wille J, van de Pavoordt EDWM, et al. Results of open pararenal abdominal aortic aneurysm repair: single centre series and pooled analysis of literature. Vascular 2017;25:234-41.
20. Cao P, Verzini F, Zannetti S, De Rango P, Parlani G, Lupattelli L, et al. Device migration after endoluminal abdominal aortic aneurysm repair: analysis of 113 cases with a minimum follow-up period of 2 years. J Vasc Surg 2002;35:229-35.
21. Chaikof EL, Blankensteijn JD, Harris PL, White GH, Zarins CK, Bernhard VM, et al. Reporting standards for endovascular aortic aneurysm repair. J Vasc Surg 2002;35:1048-60.
22. England A, Torella F, Fisher RK, McWilliams RG. Migration of the Nellix endoprosthesis. J Vasc Surg 2016;64:306-12.
23. Dorweiler B, Boedecker C, Dunschede F, Vahl CF, Youssef M. Three-dimensional analysis of component stability of the Nellix endovascular aneurysm sealing system after treatment of infrarenal abdominal aortic aneurysms. J Endovasc Ther 2017;24:201-9.
24. Lee JT, Greenberg JI, Dalman RL. Early experience with the snorkel technique for juxtarenal aneurysms. J Vasc Surg 2012;55:935-46.
25. Ullery BW, Suh GY, Lee JT, Liu B, Stineman R, Dalman RL, et al. Geometry and respiratory-induced deformation of abdominal branch vessels and stents after complex endovascular aneurysm repair. J Vasc Surg 2015;61:875-84.
26. Conway BD, Greenberg RK, Mastracci TM, Hernandez AV, Coscas R. Renal artery implantation angles in thoracoabdominal aneurysms and their implications in the era of branched endografts. J Endovasc Ther 2010;17:380-7.
27. Kandail H, Hamady M, Xu XY. Comparison of blood flow in branched and fenestrated stent-grafts for endovascular repair of abdominal aortic aneurysms. J Endovasc Ther 2015;22:578-90.
28. Boersen JT, Groot Jebbink E, Versluis M, Slump CH, Ku DN, de Vries JPM, et al. Flow and wall shear stress characterization after endovascular aneurysm repair and endovascular aneurysm sealing in an infrarenal aneurysm model. J Vasc Surg 2016;66:1844-53.
29. Basciano C, Kleinstreuer C, Hyun S, Finol EA. A relation between near-wall particle-hemodynamics and onset of thrombus formation in abdominal aortic aneurysms. Ann Biomed Eng 2011;39:2010-26.
30. Zerwes S, Nurzai Z, Leissner G, Kroencke T, Bruijnen HK, Jakob R, et al. Early experience with the new endovascular aneurysm sealing system Nellix: first clinical results after 50 implantations. Vascular 2016;24:339-47.
31. van Noort K, Overeem SP, van Veen R, et al. Apposition and positioning of the Nellix endovascular aortic aneurysm sealing (EVAS) system in the infrarenal aortic neck. J Endovasc Ther 2018;25:428-34.
32. Endologix. Nellix 3.5 Instruction for Use. Available at: www.endologix.com. Accessed September 10, 2018.

Submitted Feb 26, 2018; accepted Feb 19, 2019.